LBL-26187

Lawrence Berkeley Laboratory
UNIVERSITY OF CALIFORNIA

Accelerator & Fusion
Research Division

Center for X-Ray Optics

Presented at the Optical Society of America Meeting
on Short Wavelength Coherent Radiation:
Generation and Applications,
Cape Cod, MA, September 26–29, 1988

X-Ray Holographic Microscopy: Improved Images of Zymogen Granules

C. Jacobsen, M. Howells, J. Kirz,
K. McQuaid, and S. Rothman

October 1988

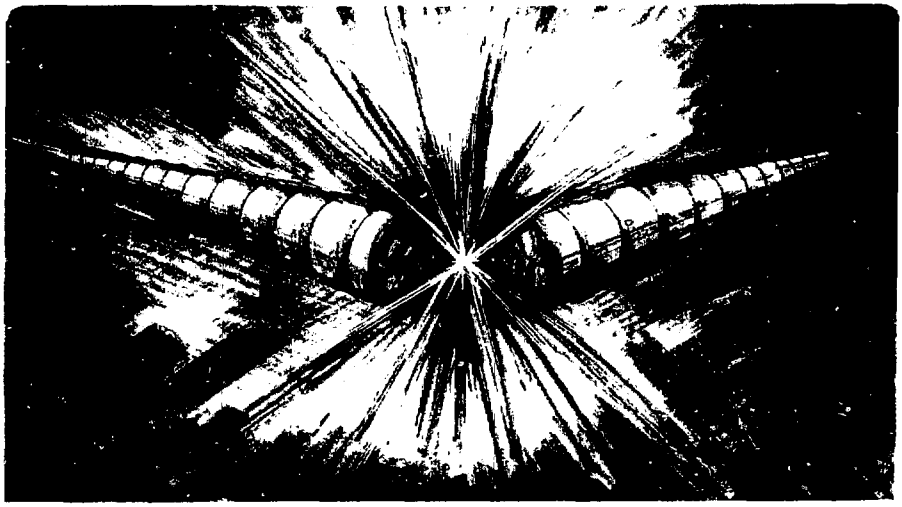

Prepared for the U.S. Department of Energy under Contract Number DE-AC03-76SF00098.

X-ray holographic microscopy: improved images of zymogen granules

Chris Jacobsen and Malcolm Howells
Center for X-ray Optics
Accelerator and Fusion Research Division
Lawrence Berkeley Laboratory
1 Cyclotron Road
Berkeley, CA 94720

LBL--26187

DE89 004783

Janos Kirz
Deptartment of Physics
State University of New York at Stony Brook
Stony Brook, NY 11794

Kenneth McQuaid and Stephen Rothman
Schools of Medicine and Dentistry
University of California, San Francisco
San Francisco, CA 94143

Soft x-ray holography has long been considered as a technique for x-ray microscopy [1]. It has been only recently, however, that sub-micron resolution has been obtained in x-ray holography [2–4]. This paper will concentrate on recent progress we have made in obtaining reconstructed images of improved quality.

The recording of our holograms has been described elsewhere [2,3]. Briefly, the holograms were recorded in November 1986 and February 1987 using $\lambda_1 = 25$ Å radiation from a N=10 period soft x-ray undulator and a temporary beamline at the National Synchrotron Light Source 2.5 GeV storage ring [5]. (This system has since been considerably upgraded, and is now returning to normal operation with a brighter undulator and a permanent soft x-ray microscopy beamline [6]). We were able to obtain a coherent soft x-ray flux of about 10^8 photons per second through the use of a grating monochromator for temporal coherence and a spatial filtering pinhole for spatial coherence. Dry specimens supported on Formvar-film-coated electron microscope grids were illuminated by plane-wave soft x-rays, and were followed at multiples of 400 μm by PMMA and/or MMA-MAA photoresists used as holographic recording media in the Gabor geometry. The photoresists were then "developed" in the solvent MIBK to convert the incident x-ray irradiance distribution to a surface relief pattern; the contrast of the relief was enhanced by vacuum evaporation of Pd:Au at 7° grazing incidence. A transmission electron microscope was then used to enlarge the holograms $\sim 2000\times$ and read out the information encoded in sub-micron fringes.

In principle, one could reduce the electron micrographs to a net hologram magnification $m \approx 250$ and then obtain reconstructions at visible wavelengths, where the wavelength ratio

$$\mu \approx \left(\frac{6000\ \text{Å}}{25\ \text{Å}}\right)$$

would match m. If the distances between the illumination source and the hologram were similarly scaled between the recording and reconstruction steps, such a reconstruction would give a magnified image with no aberrations, in what was described by Gabor as "lensless microscopy" [7]. However, our holograms contain a highly non-linear mapping of the incident x-ray intensity, which would lead to a poor signal-to-noise ratio in the reconstructed image if no corrections were made. For that reason, we have chosen to adopt a numerical approach to hologram reconstruction. By digitizing the electron micrographs with a scanning microdensitometer, we are able to obtain a numerical map of electron film density. Through the use of a simple model for the photoresist exposure, development, and readout process, an approximate mapping of film density back to incident x-ray irradiance can be made, at least for low spatial freqencies [8]. The linearized hologram is a diffracting structure which will focus an incident plane wave down to an image of the specimen (plus the "twin image" present in Gabor holography, and weak intermodulation terms). In fact, the optical reconstruction process with the original reference beam can be mimicked by computing the magnitude squared of the Fresnel transform of the hologram transmittance [9,10]. Ultimately, the power of the numerical approach lies in the fact that it allows non-linear processing algorithms such as that of Liu and Scott [11] to be used to supress the unwanted signals.

The holograms are of rat zymogen granules, which hold precursors of digestive enzymes in the pancreas. Following isolation by the standard technique [12], the granules were fixed in 1.5% glutaraldehyde in 150 mM sucrose, but were *not* stained with heavy metals in the manner which would be followed for transmission electron microscopy. The granule suspension was subsequently diluted further in sucrose, after which a micropipette was used to place a drop of the suspension on a standard 300 mesh TEM locator grid coated with ~ 100 Å of carbon-reinforced Formvar. The excess liquid was wicked away, and the grid was then air-dried, leaving occasional isolated granules and, more commonly, granule clumps on the grid.

These objects have been examined by using various conventional microscopic techniques and by x-ray holography. Figure 1 demonstrates that these unsectioned preparations are sufficiently thick to appear as opaque objects when viewed in a 100 KeV transmission electron microscope. Furthermore, their small size means that, once again, only the outlines of granules in a clump can be resolved with an optical microscope, as can be seen in Figure 2. The scanning electron micrograph of Figure 3 shows that the granule membrane remains in a spherical shape even when air-dried. Figures 1, 2, and 3 are all of different areas of the same specimen grid.

Figure 4 shows a section of a hologram and reconstructed image of the same granule clump as is shown in Figure 2. The holographic image is clearly consistent with the optical micrograph of Figure 2, except that much higher resolution information is contained in the holographic image. Fringes which would correspond to a resolution of about 500 Å are visible by inspection of the electron-microscope-enlarged hologram, and power spectra of hologram linescans suggest that information is recorded at or below the 200 Å level [3]. The reconstructed image in Figure 4 is the result of a 512^2 pixel sampling of the hologram, while Figure 5A shows a reconstructed image made from a 1024^2 pixel sampling of the same

hologram in which the diffraction-limited resolution would be 470 Å. (Because of sampling considerations, the images of Figure 5 are displayed with pixel sizes of 290 Å). Figures 5B, 5C, and 5D show the results of highpass filtering the reconstructed image to block out all information at spatial frequencies below $(2 \times 3760)^{-1}$, $(2 \times 2090)^{-1}$, and $(2 \times 990)^{-1}$ Å^{-1}, respectively. Such a filtering process means that only information at a size scale smaller than

$$\Delta_{\text{cutoff}} = \frac{1}{2 f_{\text{cutoff}}}$$

is preserved, so that Figure 5B shows only sub-3760 Å detail, Figure 5C shows sub-2090 Å detail, and Figure 5D shows only sub-990 Å detail. The Figures demonstrate that the reconstructed image contains almost exclusively sub-optical resolution information. Furthermore, granule edges clearly stand out in Figure 5D, indicating that the signal-to-noise ratio is still significant for strong sub-1000 Å detail.

Interpretation of the high-resolution information in the granule micrograph is a topic of ongoing study. As can be seen in Figure 6, a focal series of the granule shows a few "features" changing as the assumed specimen to hologram separation distance f is varied in 2 μm increments (the diffraction-limited logitudinal resolution would be 3.4 μm for this reconstruction). The changing "features" are presumably the result of focussing error aberrations, which produce contrast reversals as a coherent imaging system is brought into and then out of focus [13]. However, most high-spatial-frequency information remains unchanged in the focal series; further study will be required in order to determine whether these features are actual structures within the granules, artifacts resulting from the coherent imaging of granules stacked on top of each other, or an artifact of air-drying. Finally, it should be noted that the thickness of the granule clump is almost certainly less than the longitudinal resolution length, so that our current reconstructed images only contain two-dimensional information.

The attractions of holography as a soft x-ray imaging technique have been discussed elsewhere [14,15]. They include the ability to make use of single-shot x-ray sources if they become available at the required brightness, the fact that the focussing of the image is accomplished in the reconstruction stage (*without additional exposure to x-rays*), the natural way in which phase contrast can be utilized in holographic imaging, and the possibility of extension to diffraction tomography for achieving high-resolution, three-dimensional images. Obtaining images which show detail not visible in optical or electron microscopes gives us confidence that soft x-ray holographic microscopy is a technique with considerable potential for high resolution imaging.

Acknowledgements

We acknowledge valuable help and advice from P. Batson, J. Bastacky, J. Boland, M. Caldarolo, K. Conkling, C. Dittmore, T. Ermak, R. Feder, J. Grendell, D. Joel, T. Kondakjian, D. Pardoe, H. Rarback, and D. Sayre, as well as the generous assistance of the staff at the NSLS. This work was supported in part by the National Science Foundation under grant BBS-8618066 (J.K.) and the Director, Office of Energy Research, Office of Basic Energy Sciences, Materials Sciences Division, of the U.S. Department of Energy under contract DE-AC03-76SF00098. This work was carried out in part at the National Synchrotron

Light Source, which is supported by the Department of Energy under contract DE-AC02-76CH00016.

References

1. For summaries of preceding work, see: S. Aoki and S. Kikuta, "X-ray holographic microscopy", *Japan J. App. Phys.* **13**, 1385-1392 (1974); and M. R. Howells, M. A. Iarocci, and J. Kirz, "Experiments in x-ray holographic microscopy using synchrotron radiation", *J. Opt. Soc. Am. A* **3**, 2171-2178 (1986). A more recent review is contained in Section 4.1 of Reference 8.
2. M. Howells, C. Jacobsen, J. Kirz, R. Feder, K. McQuaid, and S. Rothman, "X-ray holography at improved resolution: a study of zymogen granules", *Science* **238**, 514-517 (1987).
3. C. Jacobsen, J. Kirz, M. Howells, K. McQuaid, S. Rothman, R. Feder, and D. Sayre, "Progress in high-resolution x-ray holographic microscopy", in D. Sayre, M. R. Howells, J. Kirz, and H. Rarback, eds., **X-ray Microscopy II** (Springer-Verlag, Berlin, 1988), pp. 253-262.
4. D. Joyeux, S. Lowenthal, F. Polack, and A. Bernstein, "X-ray microscopy by holography at LURE", in D. Sayre, M. Howells, J. Kirz, and H. Rarback, eds., **X-ray Microscopy II** (Springer-Verlag, Berlin, 1988), pp. 246-252; and D. Joyeux *et al.*, this volume.
5. H. Rarback, C. Jacobsen, J. Kirz, and I. McNulty, "The performance of the NSLS mini-undulator", *Nucl. Inst. Meth.* **A266**, 96-105 (1988).
6. C. J. Buckley *et al.*, Procedings of the 1988 International Synchrotron Radiation Instrumentation conference, Tsukuba, Japan. (To be published in *Nucl. Inst. Meth.*)
7. D. Gabor, "Microscopy by reconstructed wave-fronts", *Proc. Roy. Acad. Sci. London* **A197**, 454-487 (1949).
8. C. Jacobsen, "Soft x-ray holography microscopy of biological specimens using an undulator", Ph. D. dissertation, Department of Physics, State University of New York at Stony Brook, May 1988.
9. W. H. Carter and A. A. Dougal, "Field range and resolution in holography", *J. Opt. Soc. Am.* **56**, 1754-1759 (1966).
10. J. W. Goodman and R. W. Lawrence, "Digital image formation from electronically detected holograms", *Appl. Phys. Lett.* **11**, 77-79 (1967).
11. G. Liu and P. D. Scott, "Phase retrieval and twin-image elimination for in-line Fresnel holograms", *J. Opt. Soc. Am. A* **4**, 159-165 (1987).
12. T. H. Ermak and S. S. Rothman, "Internal organization of the zymogen granule: formation of reticular structures *in vitro*", *J. Ultrastructure Research* **64**, 98-113 (1978).
13. See e.g., Section 6-1 of J. W. Goodman, **Introduction to Fourier Optics** (McGraw-Hill Book Company, San Francisco, 1968).
14. M. R. Howells, C. Jacobsen, J. Kirz, K. McQuaid, and S. S. Rothman, "Progress and prospects in soft x-ray holographic microscopy", presented at the British Biophysical

Society Conference on Modern Microscopies, London, United Kingdom, December 20-21, 1987 (to be published).

15. C. Jacobsen, J. Kirz, M. R. Howells, and S. Rothman, "Biological microscopy via x-ray holography", presented at International Conference on 3-D Image Processing in Microscopy, Gießen, Federal Republic of Germany, March 9-11, 1988. (To be published in *European J. Cell Biology.*)

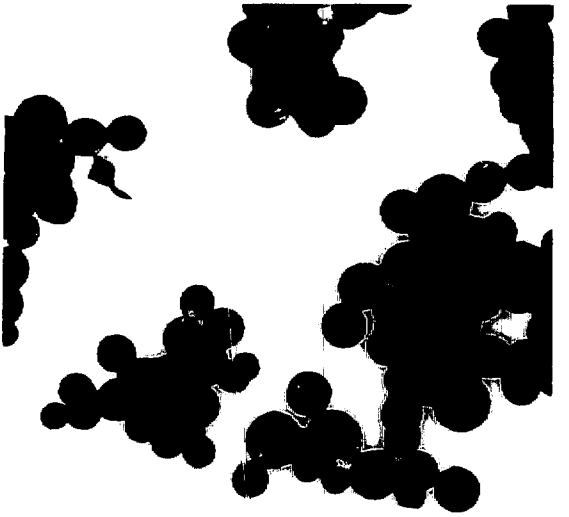

XBB 889-9071

Figure 1. Transmission electron micrograph of fixed, air dried, but unstained zymogen granules as prepared for x ray holography. The unsectioned granules are spherical with a diameter of about 0.6 μm, and thus appear opaque to a 100 KeV electron beam. Micrograph courtesy of E. Ermak.

XBB 887-7137

Figure 2. Optical micrograph of a different area of the same specimen grid as is shown in Figures 1 and 3. A 400× objective was used with a numerical aperture of 0.95; the diffraction-limited resolution of the micrograph is therefore about 0.4 μm. Therefore, only the general outline of the $\sim$ 0.6 μm-sized individual granules is visible. Because of waviness in the supporting Formvar film, the two smaller granule clumps at the bottom of the micrograph are in focus, while the larger clump at top is not. One granule clump is indicated for comparison with Figures 4, 5, and 6.

XBB 889-8947

Figure 3. Scanning electron micrograph of a different granule clump from the same specimen grid as is shown in Figures 1 and 2. The fixed, air-dried, but unstained granules (with about 50 Å of Pt sputtered onto their surface) appear as perfectly smooth spheres for the first few seconds of SEM examination; the slight "rippling" that can be seen on the granule surfaces in the Figure is the result of radiation damage from the scanned electron beam. The radiation dose required to form the SEM image is three to four orders of magnitude higher than that required to record the x-ray hologram. Micrograph courtesy of D. Pardoe and J. Bastacky.

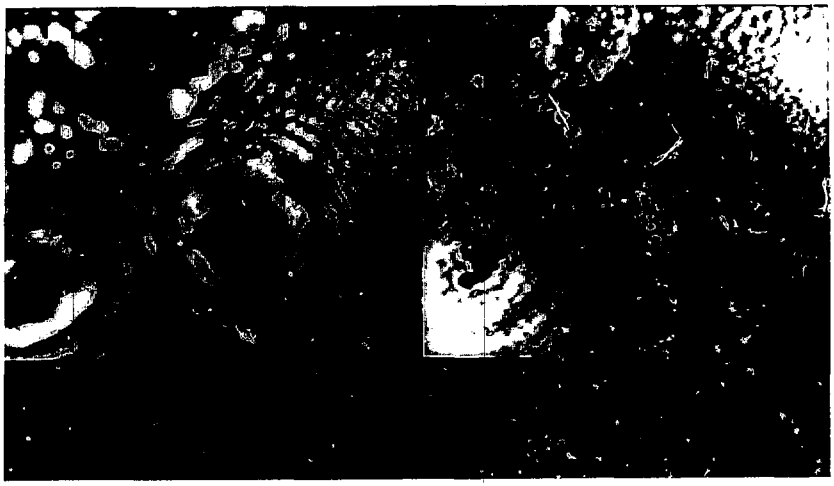

XBB 884-3072

Figure 4. Portion of an x-ray hologram (left) and its reconstructed image (right) of the same granule clump as is indicated in Figure 2. Individual granules are clearly resolved in the reconstructed image, which emerges rather dramatically from the hologram

Coulomb and surface energies. As shown in Fig. 4, an oscillation about this mode involving an amount of energy on the order of the temperature T, corresponds to a variation in the monopole - monopole term of the Coulomb energy

$$\Delta E_C = 2\sqrt{\frac{c^2 T}{k}} = 2\sqrt{pT} \qquad (9)$$

where the coefficients c and k are defined by the quadratic expansion of the total potential energy associated with the deformation mode z:

$$V(z) = B_0 + kz^2 \qquad (10)$$

and by the linearization of the Coulomb energy along the same mode:

$$E_{Coul} = E^0_{Coul} - cz. \qquad (11)$$

The quantities B_0, E^0_{Coul}, c, k and p are defined at the minimum of the total potential energy with respect to the deformation mode, and are, as a consequence, saddle-point quantities. Because of its role, illustrated in Fig. 4, p is called the "amplification parameter". An input thermal noise of the order of the temperature T is magnified in accordance to Eq. 9 and Fig. 4 giving an output kinetic energy fluctuation much greater than the temperature. This effect is probably responsible also for the great widths of the kinetic energy distributions in ordinary fission.

We are now going to consider three specific cases. The first and simplest deals in detail with only one decay mode and one amplifying mode. The decay width becomes:

$$\Gamma(\varepsilon,z)\, d\varepsilon dz \propto e^{-(\varepsilon + kz^2)/T} d\varepsilon dz . \qquad (12)$$

Remembering that the final kinetic energy can be written as:

$$E = E^0_{Coul} - cz + \varepsilon \qquad (13)$$

we can rewrite the decay width as follows:

$$\Gamma(\varepsilon,z) \propto \exp -\left[\frac{\varepsilon + (x-\varepsilon)^2/p}{T}\right] , \qquad (14)$$

where $x = E - E^0_{Coul}$.

The final kinetic energy distribution is obtained by integrating over ε:

$$P(E) \propto \int \exp -\left[\frac{\varepsilon + (x-\varepsilon)^2/p}{T}\right] d\varepsilon \qquad (15)$$

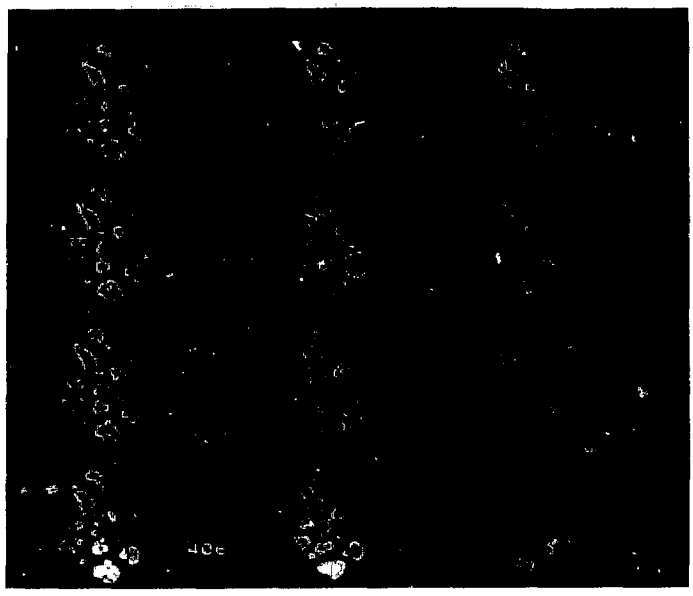

NBB 884-3073

Figure 6. A focal series of the granule clump shown in Figures 2–4. The numbers to the right of each sub-image indicate the assumed specimen-to-hologram separation distance f in μm. The focus chosen for Figures 4 and 5 was with $f = 406$ μm. As can be seen, some "features" in the image change as f is varied, presumably because they are in fact phase contrast fringes produced when an coherent imaging system is improperly focussed. Note that the diffraction-limited logitudinal resolution would be 3.4 μm for this reconstruction.